Merging Timescales and Merger Rates of Star Clusters in Dense Star Cluster Complexes

M. Fellhauer
Astronomisches Rechen-Institut, Heidelberg, Germany

H. Baumgardt
Department of Mathematics & Statistics, University of Edinburgh, Scotland, UK

P. Kroupa
Institut für theor. Astrophysik, University of Kiel, Germany

R. Spurzem
Astronomisches Rechen-Institut, Heidelberg, Germany

February 5, 2008

Abstract. Interacting galaxies like the famous Antennae (NGC 4038/4039) or Stephan's Quintet (HCG 92) show considerable star forming activity in their tidal arms. High resolution images (e.g. from HST-observations) indicate that these regions consist of up to hundreds of massive stellar clusters or tidal dwarf galaxies (TDG). In this paper we want to investigate the future fate of these clusters of massive star clusters (in this work called *super-clusters*). We simulate compact super-clusters in the tidal field of a host-galaxy and investigate the influence of orbital and internal parameters on the rate and timescale of the merging process. We show that it is possible that such configurations merge and build a dwarf galaxy, which could be an important mechanism of how long-lived dwarf satellite galaxies form. A detailed study of the merger object will appear in a follow-up paper.

Keywords: methods: numerical – galaxies: interaction – galaxies: dwarf galaxies – galaxies: star clusters – star clusters: merging

1. Introduction

High resolution images from HST-observations of the Antennae galaxies (Whitmore et al. 1999, Zhang & Fall 1999) show that the star forming regions there consist of up to hundreds of young (ages 3–7 Myr), compact massive star clusters with dimensions of a few pc. The young star clusters in the Antennae have effective radii $R_{\rm eff} = 4$ pc and masses of the order 10^4 – 10^6 $M_\odot$. These clusters are not evenly distributed but themselves clustered in super-clusters spanning regions of several hundred pc in projected diameter and have concentrated cores, i.e. the cluster-density in the centre of the super-cluster is higher than in the outer parts. The richness of the super-clusters spans from groups of only a few to super-clusters containing hundreds of new star clusters. In other systems like Arp 245, Duc et al. (2000) find a bound stellar

and gaseous object at the tip of the tidal tail. (Their numerical models show that the system is seen at approximately 100 Myr after the closest approach of the interacting pair.) This so-called tidal dwarf galaxy (TDG) contains old and new stellar material, a lot of gas and also undissolved massive stellar clusters. Systems like the merger remnant NGC 7252 (Miller et al. 1997) show a distribution of young massive star clusters which has the same age as the interaction ($\approx$ 700 Myr). All these observations show that galaxy interactions lead to the formation of new massive and compact star clusters.

Finally, galaxies like our Milky Way host several dwarf galaxies (e.g. dSph or dE) (Mateo 1999) with high specific globular cluster frequencies (Grebel 2000) and globular clusters in their tidal streams.

With this project we investigate the future fate of clusters of young massive star clusters. According to Kroupa (1998) it is possible that such configurations merge and build a dwarf galaxy. Therefore we simulate compact super-clusters in the tidal field of a host-galaxy and investigate the influence of orbital and internal parameters on the rate and timescale of the merging process (i.e. how fast the single clusters merge and how many star clusters are able to survive this process). In addition the properties of the resulting merger object and its dynamical evolution are studied. A detailed description of the properties of the merger objects will be given in a follow up paper.

2. The Simulations

The simulations are performed with the particle-mesh code SUPERBOX (Fellhauer et al. 2000). In SUPERBOX densities are derived on Cartesian grids using the nearest-grid-point scheme. From these density arrays the potential is calculated via a fast Fourier-transformation. The particles are then integrated forward in time using a fixed time-step Leap-Frog algorithm. SUPERBOX has a hierarchical grid architecture which includes for each object two levels of high-resolution sub-grids. These sub-grids stay focused on the objects and travel with them through the simulation space, providing high resolution at the places of interest (in this case the super-cluster and the single clusters within).

The massive star clusters are simulated as Plummer-spheres containing 100,000 particles each, having a Plummer-radius of $R_{\rm pl} = 6$ pc and a cutoff radius $R_{\rm cut} = 30$ pc. Each cluster has a total mass of $M_{\rm cl} = 10^6$ M$_\odot$ and a crossing time of 1.4 Myr.

The super-cluster is also modelled as a Plummer distribution made up of N_0 star clusters described above, has a Plummer-radius $R^{\rm sc}_{\rm pl}$ and cutoff radius $R^{\rm sc}_{\rm cut} = 6R^{\rm sc}_{\rm pl}$. The Plummer-radius of the super-cluster has

values of 50, 75, 150 and 300 pc. In this project the number of clusters is kept constant at $N_0 = 20$, which is a typical number of star clusters found in these super-clusters. N_0 was chosen small enough to get results with a considerable amount of CPU-time. Higher values of N_0 will be dealt with using the newly available parallel version of SUPERBOX in the near future. In our calculations the super-clusters have an initial velocity-distribution according to the Plummer-distribution we gave them (i.e. they are initially in virial equilibrium).

The super-cluster orbits through the external potential of a parent galaxy, which is given by

$$\Phi(r) \;=\; \frac{1}{2}\; v_{\rm circ}^2 \cdot \ln\left(R_{\rm gal}^2 + r^2\right) \tag{1}$$

with $R_{\rm gal} = 4$ kpc and $v_{\rm circ} = 220$ km/s. We refer the reader to Kroupa (1998), who describes the isolated case. The centre of the super-cluster moves on a circular orbit at distance D around the centre of the galaxy. The distance D from the galactic centre is varied to be 5, 10, 20, 30, 50 and 100 kpc.

The tidal radius R_t of the super-cluster depends mainly on D, but has also a low dependency on $R_{\rm pl}^{\rm sc}$. R_t lies at the local maxima of $\Phi_{\rm eff}$. It can be derived numerically by setting $\partial\Phi_{\rm eff}/\partial r = 0$ where $\Phi_{\rm eff}$ is

$$\begin{aligned}\Phi_{\rm eff}(r) \;=\; & \frac{1}{2}\; v_{\rm circ}^2 \cdot \ln\left(R_{\rm gal}^2 + r^2\right) \;-\; \frac{GM}{R_{\rm pl}^{\rm sc}} \cdot \left(1 + \left(\frac{r-D}{R_{\rm pl}^{\rm sc}}\right)^2\right)^{-1/2} \\ & - \frac{1}{2}\left(\frac{v_{\rm circ.orb.}}{D} \cdot r\right)^2 .\end{aligned} \tag{2}$$

The grids in this project are chosen to have 64^3 mesh-points with the following sizes:

- The innermost grids cover single star clusters and have sizes $(2 \cdot R_{\rm core})$ of 60 pc. This gives a resolution of 1 pc per cell.

- The medium grids have sizes $(2 \cdot R_{\rm out})$ approximately equal to the cut-off radius of the super-cluster $(R_{\rm cut}^{\rm sc})$ to ensure that every star cluster is in the range of the medium grid of every other cluster. This means the medium grids have the sizes shown in Table I

- The outermost grid (size: $2 \cdot R_{\rm system}$) covers the orbit of the super-cluster around the galactic centre. This means $2 \cdot R_{\rm system}$ is chosen to be 10 kpc larger than $2 \cdot D$, where D is the distance of the super-cluster from the galactic centre.

Table I. Grid sizes and resolutions per cell of the medium grids.

$R^{\rm sc}_{\rm cut}$	$2 * R_{\rm out}$	resolution
300 pc	600 pc	10.0 pc
450 pc	1,000 pc	16.7 pc
900 pc	2,000 pc	33.3 pc
1,800 pc	3,000 pc	50.0 pc

The two-dimensional parameter-space of our simulations ($R^{\rm sc}_{\rm pl}$ and D) can also be described with two dimensionless variables, namely

$$\alpha \; = \; R_{\rm pl}/R^{\rm sc}_{\rm pl} \qquad\qquad \beta \; = \; R^{\rm sc}_{\rm cut}/R_t \tag{3}$$

α describes how densely the super-cluster is filled with star clusters. β describes the strength of the tidal forces acting on the super-cluster.

Table II lists the dimensionless parameters α and β for the different choices of the physical quantities $R^{\rm sc}_{\rm pl}$ and D.

Table II. Dimensionless parameters as function of the physical quantities.

α	$R^{\rm sc}_{\rm pl}$ [pc]				β	$R^{\rm sc}_{\rm pl}$ [pc]			
D [kpc]	50	75	150	300	D [kpc]	50	75	150	300
5	0.12	0.08	0.04		5	0.775	1.178	2.500	
10	0.12	0.08	0.04		10	0.617	0.932	1.935	
20	0.12	0.08	0.04	0.02	20	0.419	0.630	1.282	2.761
30	0.12	0.08	0.04	0.02	30	0.323	0.486	0.981	2.048
50	0.12	0.08	0.04	0.02	50	0.232	0.348	0.700	1.431
100				0.02	100				0.89

For each combination of (α, β) several (3–6) random realisations are performed. Results discussed later for one pair of the parameter set are computed mean values out of the different simulations. Our study covers more than the observed ranges of parameters to show the influences of the different parameters more clearly.

This is a first theoretical and numerical approach to investigate the fate of the super-clusters. Although, in nature, it is unlikely that two star clusters form overlapping but with uncorrelated velocities, we do not reject random number placements which put two clusters in a

distance where they already overlap. Our simulations do not include gas dynamics, therefore they are valid after the expulsion of gas from the star clusters. By that time, clusters in the centre could already overlap each other.

3. Results

The number of star clusters in the super-cluster decreases due to two concurrent processes. The first and also the most important one is the merging process. The second one is the escape of star clusters from the super-cluster. Escape plays an important role only on long timescales or if the super-cluster is larger than its tidal radius (i.e. $\beta > 1$).

$$N(t) \;=\; N_0 - n_{\rm m}(t) - n_{\rm esc}(t) \tag{4}$$

where $n_{\rm m}$ is the number of merged clusters and $n_{\rm esc}$ the number of escaped clusters.

3.1. Merging Timescales

In our simulations the timescale of the merger process is very short. Most cluster merge within the first few crossing times of the super-cluster, forming a dense and spherical merger object in the centre of the super-cluster.

To determine the timescale of this merger process we first have a look at simulations with $\beta < 1.0$. With this restriction we can neglect the number of escaping clusters (i.e. $n_{\rm esc}(t) \equiv 0$).

Then we take the following ansatz for the decrease of the number of clusters. If a star cluster makes one crossing through the super-cluster the chance to meet and merge with another cluster is the area covered by the cross-sections of all other clusters divided by the area of the super-cluster. We therefore define the merger-rate R (number of merger events per dimensionless time unit) as the ratio between the cross-sections of all (N) star clusters ($A_{\rm hit}$) travelling through the super-cluster and the area of the super-cluster $A_{\rm sc}$. The merger rate R per $T_{\rm cr}^{\rm sc}$ (crossing time of the super-cluster) should therefore be given by

$$R \;=\; -\frac{{\rm d}N}{{\rm d}\tau} \;=\; N \cdot \frac{A_{\rm hit}}{A_{\rm sc}} \tag{5}$$

with

$$\tau \;=\; \frac{t}{T_{\rm cr}^{\rm sc}} \tag{6}$$

being a dimensionless time and

$$\begin{aligned} A_{\rm sc} &= \pi \cdot (R^{\rm sc}_{\rm cut,eff})^2 \\ &= \pi \cdot (\gamma \cdot R^{\rm sc}_{\rm pl})^2 \end{aligned} \tag{7}$$

is the projected area of the super-cluster with a mean radius that includes all clusters. This radius is smaller than $R^{\rm sc}_{\rm cut}$ due to the fact that the super-clusters contain only a limited number of clusters. In our simulations we find that γ is given by $\gamma = 3.8 \pm 0.1$.

For the cross-sections of all clusters we take the ansatz (see also Fig. 1)

$$\begin{aligned} A_{\rm hit} &= (N-1) \cdot A_{\rm cl} \qquad \text{with} \\ A_{\rm cl} &= \pi \cdot r_{\rm m}^2 \end{aligned} \tag{8}$$

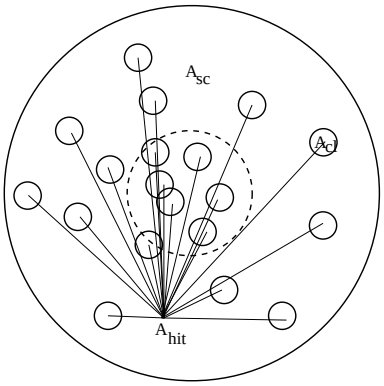

Figure 1. Schematic view of the first ansatz to determine the merging timescales.

Every star cluster sees the cross-section $A_{\rm cl}$ of $N-1$ other clusters and $r_{\rm m}$ being the maximum distance at closest approach which leads to a merger afterwards. R is then proportional to N^2 and the number of clusters $N(\tau)$ should decrease with time proportional to $1/(1+k\tau)$.

To determine $A_{\rm cl}$ we first have to check how the average encounter between two star clusters (or a star cluster and the merger object) looks like. Therefore we have to check the relative velocities and separations at the point of closest approach, which afterwards leads to the merging of the two star clusters. Fig. 2 shows the relative separation between a particular star cluster and the merger object. One can clearly see that the two objects are separated at their first encounter, implying the distance at closest approach is larger than the mean square radius of a single cluster. Their relative velocity is larger than the average velocity inside the super-cluster but less than a factor of three. Because even

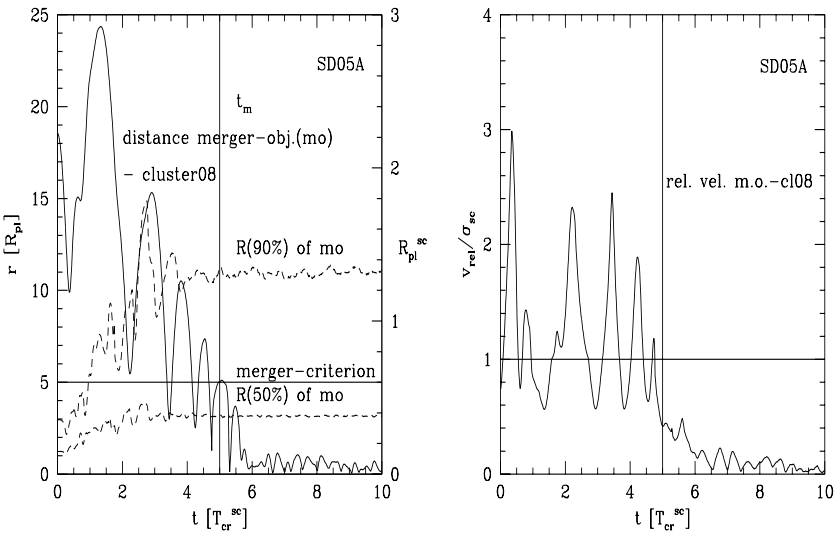

Figure 2. A typical example for the merging of a star cluster with the merger object. Left panel: Solid line shows the distance between the merger object and the star cluster. Dashed lines show the half-mass- and the 90%-radii of the merger object. Horizontal line marks the maximum distance for the merger-criterion – if the distance of two objects stays less than this for the rest of the simulation the two objects are assumed to be merged; vertical line shows the adopted merger-time $t_{\rm m}$. Right panel: Ratio between the relative velocity $v_{\rm rel}$ of the cluster and the merger object and the velocity dispersion $\sigma_{\rm sc}$ of the super-cluster.

head-on encounters do not lead to merging if the encounter velocity lies above a certain treshhold, we follow a simple criterion extracted from Gerhard & Fall (1983 their Fig. 1)

$$2 \cdot \sigma_{\rm sc}^2 \;\leq\; \frac{GM_{\rm cl}}{R_{\rm pl}} \tag{9}$$

where $\sqrt{2}\sigma_{\rm sc}$ is the typical relative velocity of a pair of star clusters. This equation holds for $\alpha \leq 0.085$. For $\alpha > 0.085$ we argue below that in our parameter range we already start with a merged object in the centre of the super-cluster, and therefore $M_{\rm cl}$ has to be replaced by $\nu M_{\rm cl}$ where ν is the number of merged central clusters. With $\nu \geq 2$ and increasing with increasing α, Eq. 9 holds for all values of α in our parameter space.

In this paper, we define two clusters as merged if their mutual distance stays smaller then five Plummer-radii $R_{\rm pl}$ for the rest of the simulation. We found that $5\,R_{\rm pl}$ is a good compromise between declar-

ing no cluster as merged (the merger criterion being chosen too small) and merging all clusters right form the beginning (their mean distance being smaller than the merger criterion). Smaller merger radii have problems in the late stages of the simulation, where the centres of density of dissolved clusters are very hard to determine and could be found off-centre of the extended merger object. If the merger radius is chosen too small, these clusters would not be counted as merged. An energy criterion has to be handled with care, because clusters may be bound to the merger object without merging but staying on a circular orbit and decaying on the dynamical friction timescale.

The next step is to approximate the energy gain of the clusters due to the passage. Aguilar & White (1985) showed that the total energy exchange in the tidal approximation given by Spitzer (1958),

$$\Delta E \;=\; \frac{1}{2}\; M_{\rm cl} \left(\frac{2GM_{\rm cl}}{r_{\rm p}^2 v_{\rm p}} \right)^2 \;\frac{2}{3} r_{\rm c}^2, \tag{10}$$

gives reasonable results if $r_{\rm p} \geq 5r_{\rm c}$. In this formula $r_{\rm c}$ denotes the mean square radius of a single cluster. With a cut-off of $6R_{\rm pl}$ we calculate the mean square radius of a Plummer-sphere as approximately $1.5R_{\rm pl}$ which gives $r_{\rm c}^2 \approx 2.3R_{\rm pl}^2$. Fig. 2 shows that the two objects pass each other for the first time at a distance which holds for the criterion of Aguilar & White. $r_{\rm p}$ and $v_{\rm p}$ are the distance and the velocity at the point of closest approach. If we assume that $v_{\rm p}$ is equal to the mean relative velocity of two clusters in the super-cluster, $\sqrt{2}\sigma_{\rm sc}$, i.e. we neglect gravitational focusing and the acceleration of the star clusters firstly and taken into account that both clusters are able to gain energy we get

$$\Delta E \;=\; 2\frac{4 \cdot 2.3}{3 \cdot 2} \frac{G^2 M_{\rm cl}^3 R_{\rm pl}^2}{r_{\rm p}^4 \sigma_{\rm sc}^2}. \tag{11}$$

To obtain the critical impact parameter which leads to a merger, we set the energy exchange equal to the orbital energy of the two clusters in the super-cluster: $\Delta E = \frac{1}{4}\; M_{\rm cl}\; (\sqrt{2}\sigma_{\rm sc})^2$. Inserting for $\sigma_{\rm sc}$ the mean velocity of "particles" in a Plummer-sphere

$$\sigma_{\rm sc}^2 = \frac{3\pi}{32} \frac{GM_{\rm sc}}{R_{\rm pl}^{\rm sc}} \tag{12}$$

with $M_{\rm sc} = N_0 M_{\rm cl}$ and using the definition of α from Eq. 3, one obtains for $r_{\rm p}$

$$r_{\rm p} \;=\; \left(\frac{8 \cdot 32^2 \cdot 2.3}{3(3\pi)^2 N_0^2} \right)^{1/4} \cdot \sqrt{\alpha} \cdot R_{\rm pl}^{\rm sc} \;\approx\; 0.65\sqrt{\alpha} \cdot R_{\rm pl}^{\rm sc}. \tag{13}$$

In this formula we have not taken into account that the clusters are gravitationally focused. Inserting Spitzers (1987; eq. 6-15) formula for gravitational focusing,

$$r_{\rm m} \;=\; r_{\rm p}\sqrt{1.0+\frac{4GM_{\rm cl}}{r_{\rm p}(\sqrt{2}\sigma_{\rm sc})^2}}, \tag{14}$$

we obtain

$$r_{\rm m} \;=\; 0.65\cdot\sqrt{\alpha}\cdot\sqrt{1.0+\frac{0.52}{\sqrt{\alpha}}}\cdot R_{\rm pl}^{\rm sc}. \tag{15}$$

Given the values of α of our simulations we derive the values for $r_{\rm m}$ given in Table III. The merger rate R is then

Table III. Merger radius $r_{\rm m}$ in units of $R_{\rm pl}^{\rm sc}$ and $R_{\rm pl}$ and proportionality factor δN_0 for the different α-values.

α	0.24	0.12	0.08	0.04	0.02	0.006
$r_{\rm m}$ $[R_{\rm pl}^{\rm sc}]$	0.46	0.36	0.31	0.25	0.20	0.14
$r_{\rm m}$ $[R_{\rm pl}]$	1.91	2.97	3.88	6.18	9.96	23.4
$\delta(\alpha)\cdot N_0$	0.29	0.18	0.13	0.087	0.055	0.027

$$R \;=\; N\cdot(N-1)\cdot\frac{(0.65)^2\alpha(1+\frac{0.52}{\sqrt{\alpha}})}{\gamma^2} \;\approx\; \delta(\alpha)\cdot N^2. \tag{16}$$

Solving for $R=-{\rm d}N/{\rm d}\tau$ gives

$$N(\tau) \;=\; N_0\cdot\frac{1}{1+\delta(\alpha)N_0\tau}, \tag{17}$$

with the values for $\delta(\alpha)\cdot N_0$ shown in Table III. This dependency is plotted as dashed lines in Figs. 3 & 7.

On the other hand, using instead the merger criterion by Aarseth & Fall (1980) as described in Gerhard & Fall (1983),

$$\frac{r_{\rm p}^2}{[4R_{\rm h}]^2}+\frac{v_{\rm p}^2}{[1.16v_{\rm esc}(p)]^2} \;\leq\; 1, \tag{18}$$

(their Eq. 4) where

$$v_{\rm esc}(p)^2 \;=\; \frac{4GM_{\rm cl}}{(r_{\rm p}^2+2R_{\rm pl}^2)^{1/2}}, \tag{19}$$

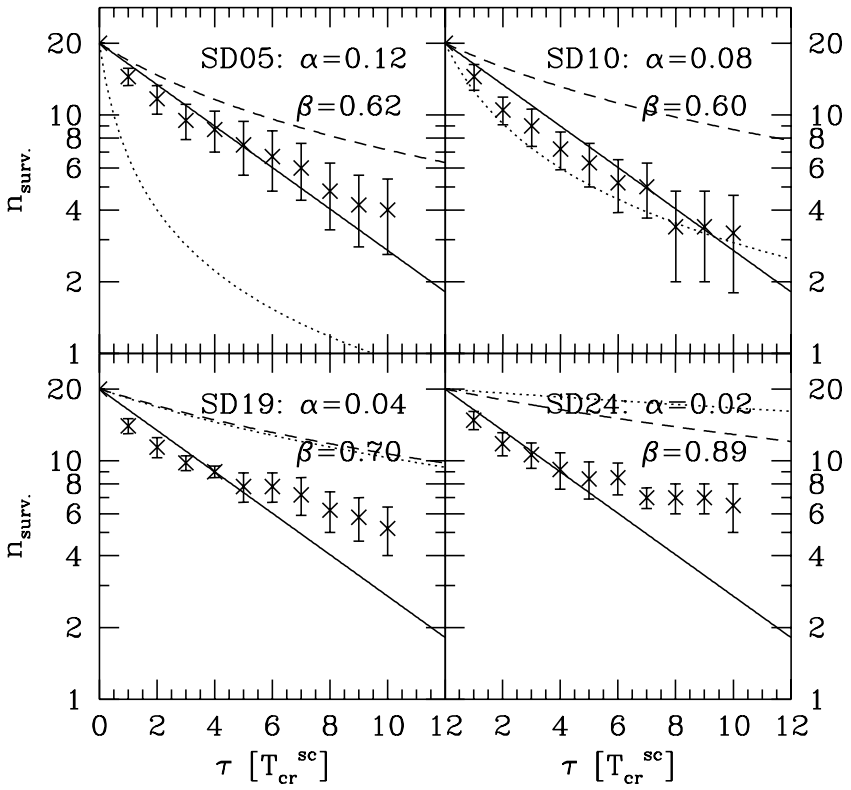

Figure 3. Number of remaining objects vs. time measured in crossing times of the super-cluster for different values of the parameter α. β is kept smaller than 1.0. Lines show theoretical curves. Solid line corresponds to an exponential decrease, dashed line shows the $1/(1+k\tau)$-decrease which depends on α. Dotted lines rely on the Aarseth & Fall criterion (Eq. 20).

(their Eq. 5) with $R_{\rm h}$ being the half-mass radius of a Plummer-sphere ($\approx 1.3 R_{\rm pl}$) and $v_{\rm p} = \sqrt{2}\sigma_{\rm sc}$ we obtain

$$r_{\rm p} \;\leq\; \left(27.04 + 67.6\sqrt{671.75\alpha^2 + 22.31}\cdot\alpha + 1754.79\cdot\alpha^2\right)^{1/2} \cdot \alpha\; R_{\rm pl}^{\rm sc} \quad (20)$$

Using $r_{\rm p}$ from this expression instead of $r_{\rm m}$ in our Eq. 8 we obtain the dotted curves in Figs. 3 & 7. We note that this ansatz does not lead to a good description of our results. It leads to an α dependency of $r_{\rm p} \propto \alpha^2$, which is steeper than we find in our simulations. Also the merger theory

of Makino & Hut (1997) does not agree with our results. They find a dependency on α with a power of 1.5, which does not fit our data. In our simulations we find a very weak dependency of the merging timescales on the parameter α. For our main parameter range ($\alpha = 0.02-0.12$) there is even no visible dependency. The simulations show a clear exponential decrease of the number of clusters with dimensionless time τ independent of the choice of α (see Fig. 3). Therefore, a merger theory depending on the merging of single clusters must be wrong.

The mean projected distance of clusters inside the innermost Plummer radius of the super-cluster depends only on the choice of N_0 and is given by

$$d_{\rm mean}(1R_{\rm pl}^{\rm sc}) \;=\; \kappa \cdot \sqrt{\frac{\pi (R_{\rm pl}^{\rm sc})^2}{N_{\rm proj}}}. \tag{21}$$

Numerical simulation shows that κ is given by 0.53. Since half the star clusters lie within one projected Plummer radius, we get for our choice of $N_0 = 20 \rightarrow N_{\rm proj} = 10$

$$d_{\rm mean}(1R_{\rm pl}^{\rm sc}) \;\approx\; 0.30 R_{\rm pl}^{\rm sc}. \tag{22}$$

Comparing this value with the merger radii $r_{\rm m}$ for our choices of α (see Table III) one can see that in the centre of the super-cluster the mean distance between two clusters (within the innermost Plummer-radius $R_{\rm pl}^{\rm sc}$) is comparable the merger radius for most α. In the centre the clusters are not able to separate from each other right from the beginning and the merging of them should therefore happen very quickly within one or two crossing times of the super-cluster, especially for high α.

In this case we have to deal with a big merger object covering the central area of the super-cluster. Merging happens preferably with this central object. Therefore, our ansatz for $A_{\rm hit}$ in Eq. 8 fails. Instead we use the following ansatz shown in Fig. 4. The merging cross-section $A_{\rm hit}$ is now a fraction ϵ of the area of the whole super-cluster $A_{\rm sc}$

$$A_{\rm hit} \;=\; \epsilon A_{\rm sc}. \tag{23}$$

which has to be determined. Inserting in Eq. 5 ($R = -{\rm dN}/{\rm d}\tau = \epsilon {\rm N}$) and integrating leads to

$$N(\tau) \;=\; N_0 \cdot \exp(-\epsilon\tau). \tag{24}$$

The exponential decrease, according to Eq. 24, is plotted in Fig. 3 as the solid lines. There one sees clearly that the number of clusters first decreases exponentially. One should also notice that the merging timescale is now independent of the choice of α.

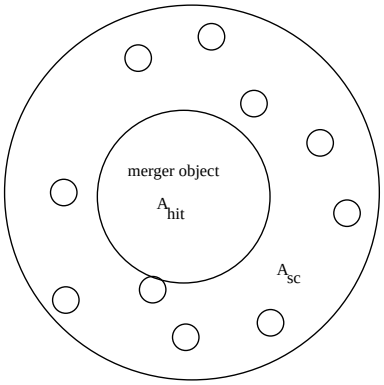

Figure 4. Schematic view of the new ansatz to determine the merging timescales.

After all clusters travelling through the centre have merged with the central merger object, the further decrease of N with time levels off. This is due to the fact that even if $\beta < 1.0$ there is the chance that some clusters escape and as a second effect there are clusters on rather circular orbits which do not travel through the central area. In low α cases ($\alpha = 0.04, 0.02$) these clusters do not merge but their orbits will decay on timescales of the dynamical friction.

To prove the independency on α we consider two characteristic quantities, namely the mean merger rate within the first crossing time ($R_{1.T_{\rm cr}^{\rm sc}}$) and the half-life merging time ($T_{1/2}$), i.e. the dimensionless time until $N_0/2$ of the clusters have merged. Fig. 5 shows the number of clusters merging within the first crossing time, and the time it takes to merge half the clusters. All simulations with the same α, and which have $\beta < 1$, are binned together. As can be seen, there is no dependency on α.

The mean merger rate within the first crossing time and the mean half-life merging time derived from our simulations are given by

$$\begin{aligned} R_{1.T_{\rm cr}^{\rm sc}} &= 3.90 \pm 0.32 \ [\text{merger events}/T_{\rm cr}^{\rm sc}] \\ T_{1/2} &= 4.18 \pm 0.35 \ [T_{\rm cr}^{\rm sc}] \end{aligned} \tag{25}$$

are plotted in Fig. 5 and are also displayed in Fig. 6. Inserting this values in our ansatz (Eq. 23) for the merging times gives

$$\epsilon \approx 0.2. \tag{26}$$

Fig. 6 shows the mean values of $R_{1.T_{\rm cr}^{\rm sc}}$ and $T_{1/2}$ for all combinations of (α, β). It is clearly visible that there is no dependency of the results on β at all. It therefore seems that β influences the number of clusters which are able to merge rather than the timescale of the merger process.

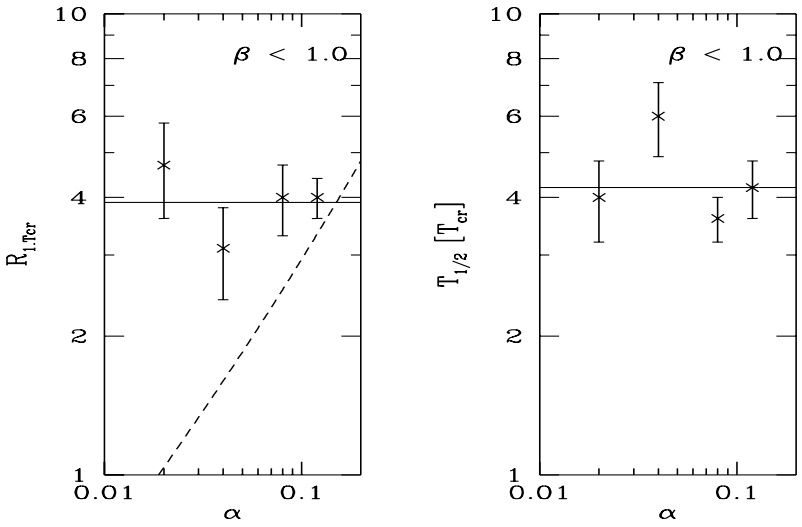

Figure 5. $R_{1.T_{\rm cr}^{\rm sc}}$ and $T_{1/2}$ as function of α for all simulations with $\beta < 1$. Solid lines show mean values from Eq. 25 while dotted line corresponds to the α-dependent theory from Eq. 16.

We expect to obtain a change in the initial behaviour of the system if $r_{\rm m}$ falls well below the mean projected distance of the clusters. For our choice of N_0, this should happen approximately for $\alpha \leq 0.02$. Then our first ansatz (Eq. 5) should represent the system. On the other hand if α becomes higher than ≈ 0.2, the mean distance of all clusters is smaller than the merger radius – all N_0 star clusters should then merge within one or two crossing times. To prove this behaviour we performed test calculations without tidal field. The results (Fig. 7) show nicely the transition between these three regimes. The upper left panel is a simulation with $\alpha = 0.24$ and one sees clearly that almost all clusters merge within the first two crossing times. In the lower right panel a simulation with $\alpha = 0.006$ is displayed. The number of clusters decreases according to our α-dependent theory.

3.2. Merger-Rates

The number of clusters, $n_{\rm m}$, which end up in the merger object shows no significant dependency on α and β, as long as the super-cluster configuration is well inside it's tidal radius (i.e. $\beta < 1.0$). In this case

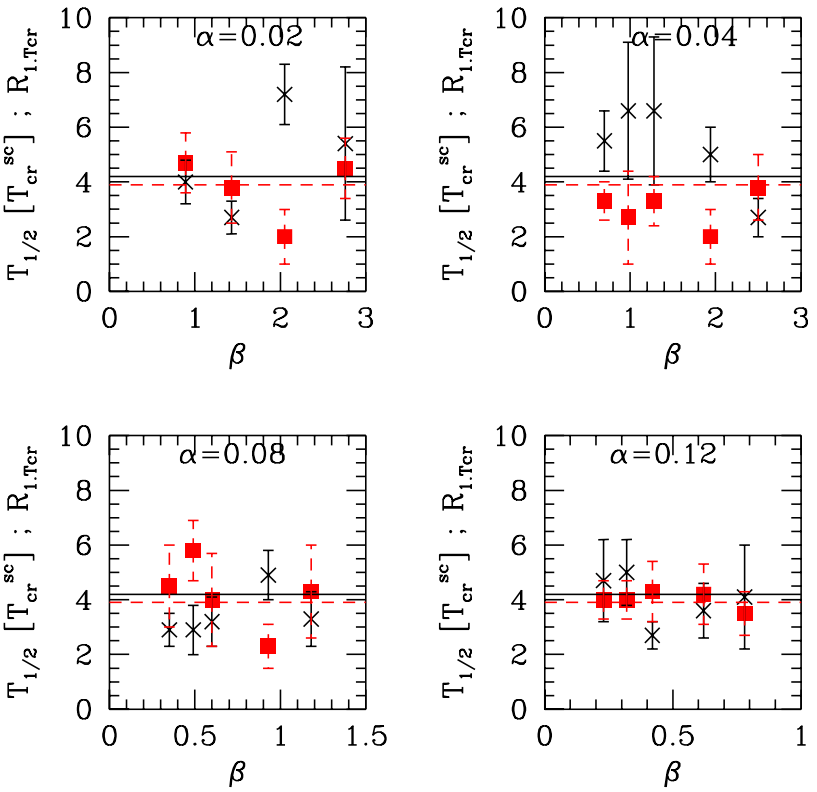

Figure 6. $R_{1.T_{\rm cr}^{\rm sc}}$ (boxes) and $T_{1/2}$ (crosses) as a function of β for the different choices of α. Solid line is the mean value for $T_{1/2}$, dashed line for $R_{1.T_{\rm cr}^{\rm sc}}$ from Eq. 25.

almost all clusters merge and only one or two clusters sometimes survive by chance. As one can see in Fig. 8, $n_{\rm m}$ is close to $N_0 = 20$.

This changes if β becomes larger than 1. There is a significant drop in $n_{\rm m}$ which also shows a weak α-dependency.

We interpret this result as follows: We start with Eq. 4 and neglect the rare case of an escaping merged cluster here. If β is small ($\beta < 1$) tidal effects are not dominant, and the evolution of $N(t)$ is determined by the merger processes alone as discussed before. If $\beta > 1$ there is a trend that clusters can leave the super-cluster before participating in the merger events. The number of escaping clusters depends on how many clusters initially are outside the tidal radius and on the individual velocities of such clusters. With only 20 clusters initially for

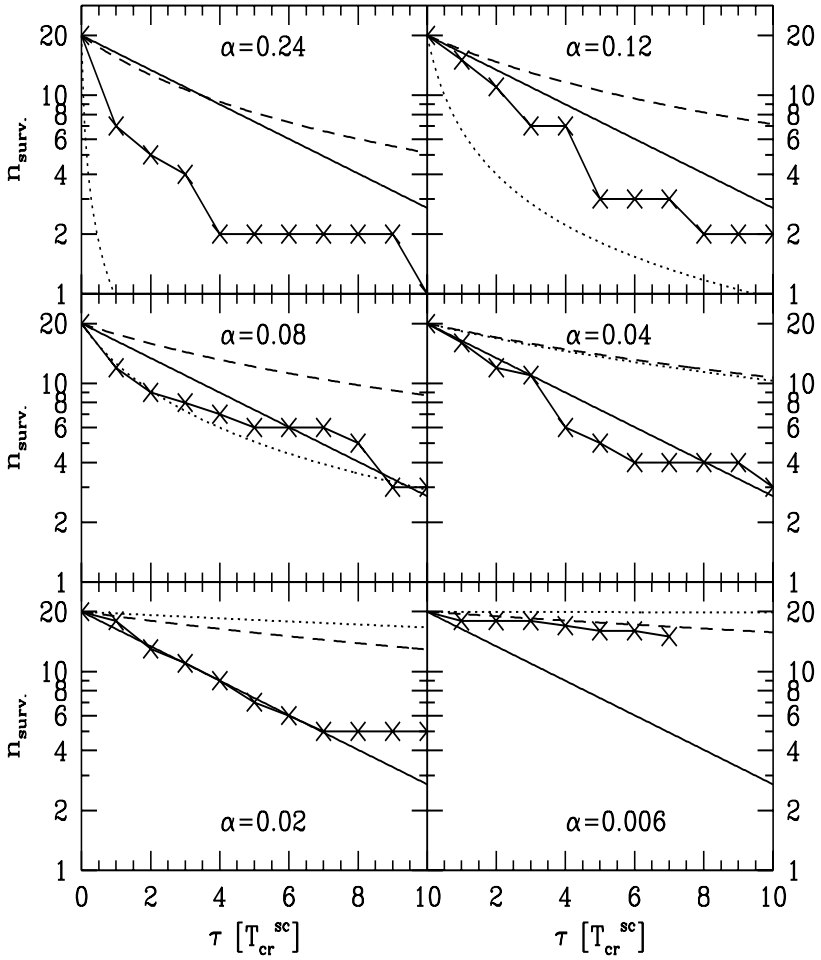

Figure 7. Same as Fig 3 but without tidal field and more extended α-range. Errorbars are omitted because only one simulation for each α-value was performed.

the entire super-cluster any statistics of the subset of escaping clusters is extremely poor. Their number strongly depends on the random numbers used for the initialisation of the system. Keeping in mind this poor statistical weight of our data, we nevertheless identify two physically reasonable trends in Fig. 8: first, the larger β, the smaller the number of

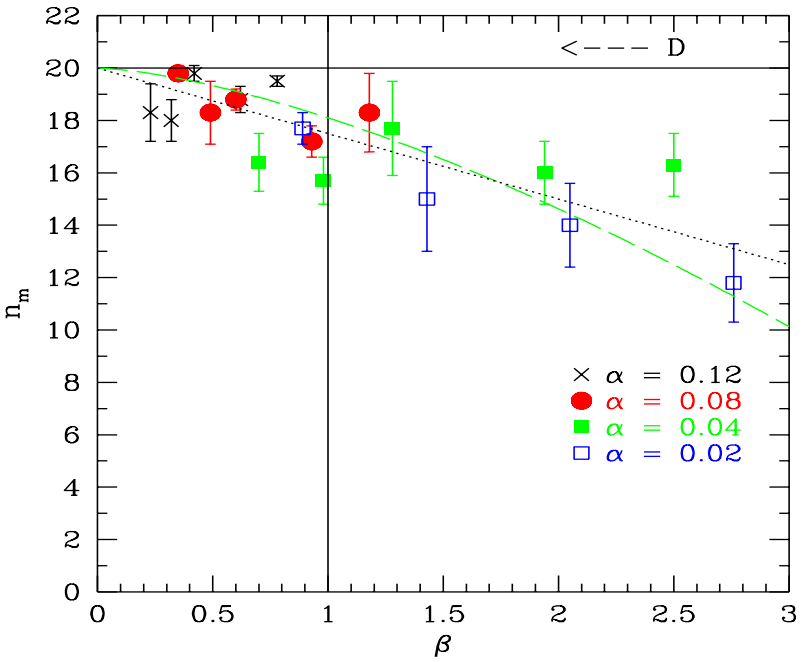

Figure 8. Number of merged clusters $n_{\rm m}$ vs. parameter β for different values of α.

merging clusters, and second, this trend is more pronounced for small α. This result is consistent with the picture that strong tidal fields lead to more escapers (i.e. less clusters available for merging); if, however, the individual clusters are relatively extended (larger α), the merging competes with the escape; clusters on orbits of potential escapers could be captured in the central regions by merging with a higher probability.

Binning the simulations in 5 β-bins, as shown in Fig. 9, shows that the dependency on β is linear. As best-fit for the data of our simulations we calculate

$$n_{\rm m} \;=\; 20 - (2.5 \pm 0.1) \cdot \beta. \qquad (27)$$

To advance that kind of reasoning to an extreme, we could compare our results with the findings of Baumgardt (1998), who models the escaping stars from star clusters. He proposes a $\beta^{3/2}$-dependency. Our results are consistent with Baumgardt's results, in particular for $\alpha \to 0$ in which case $N(\tau) \to N_0$ in Eq. 17 (where $n_{\rm esc}$ was neglected), so that

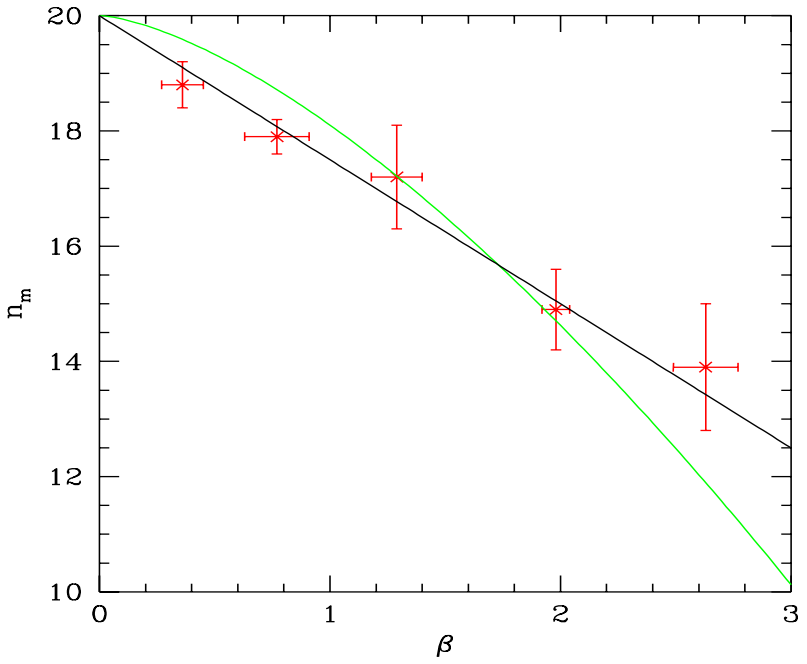

Figure 9. Number of merged cluster as function of β. Simulations are put together in 5 β-bins. Straight line is the fitted linear decrease; curved line would be the theoretical $\beta^{3/2}$-dependency as stated in Baumgardt (1998).

$N(t) \rightarrow N_0 - n_{\rm esc}(t)$ (Eq. 4). Note, however, that our particle number is very small compared to that work.

3.3. Building Up the Merger Objects

The formation scenario of the merger object depends on the chosen α-value. One finds that with high values of α, one has overlapping star clusters at the centre right from the beginning, and the simulation already starts with a merger object in the centre of the super-cluster. With decreasing values of α, the merger-tree starts with the merging of clusters at different positions in the super-cluster. Afterwards, these merger objects sink to the centre and merge together. The exact details of the merging depend however on the starting conditions, and there can always be cases with high α behaving like low α and vice versa.

Fig. 10 and 11 show some snapshots of the evolution of clusters with high and low α-values.

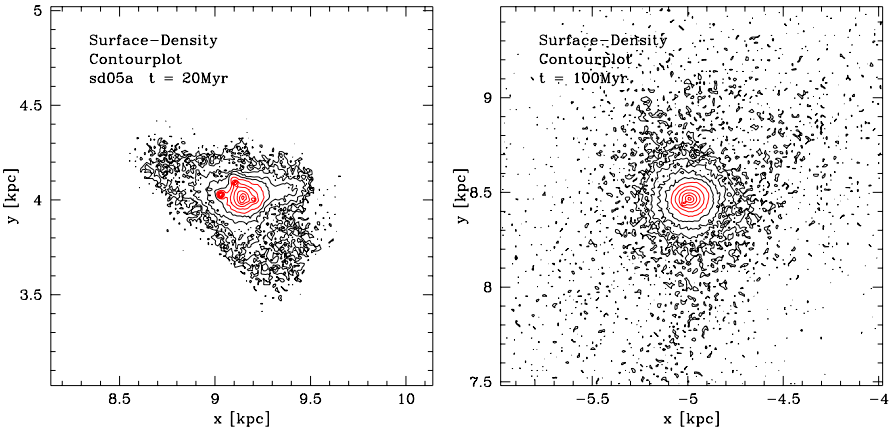

Figure 10. Surface-density contour plots (resolution: $(10\ \mathrm{pc})^2$) of a simulation with $\alpha = 0.12$ and $D = 10$ kpc. The crossing time of the super-cluster is 7.4 Myr. High values of α correspond to compact super-clusters with short crossing times.

Since the crossing-time of the super-cluster expressed in physical units depends on its size and therefore on α, the merger rates, if expressed in Myrs, also depend on α: Large α-values correspond to compact clusters which merge within a few tens of a Myr, while small α-values correspond to extended clusters in which it can take up to 1 Gyr until all clusters are finally merged.

After 20 Myr almost every cluster has already fallen into the merger object at the high α simulation (Fig. 10). At $t = 100$ Myr only the last single cluster can be seen (as a disturbance in the contours) merging with the main object.

In the low α simulation (Fig. 11) almost every cluster is seen as an individual object, even after 100 Myr. After 1 Gyr the merger object is surrounded by clusters which are still in the process of merging. These clusters may account for a high specific cluster frequency of the merger object. Not shown in the last snapshot are the 2 escaping clusters travelling on the same orbit around the galaxy as the merger object.

The merger objects show an exponential density distribution with exponential scale-length $r_{\mathrm{exp}} \approx 10$ pc and follow a de-Vaucouleur surface density profile with line-of-sight velocity dispersions about 20 km/s. A detailed description and analysis of our merger-objects is subject of Fellhauer (2000) and a follow-up paper. Here we merely briefly note that our merger objects fall in the region between dwarf galaxies and globular clusters in the central surface brightness – absolute magnitude

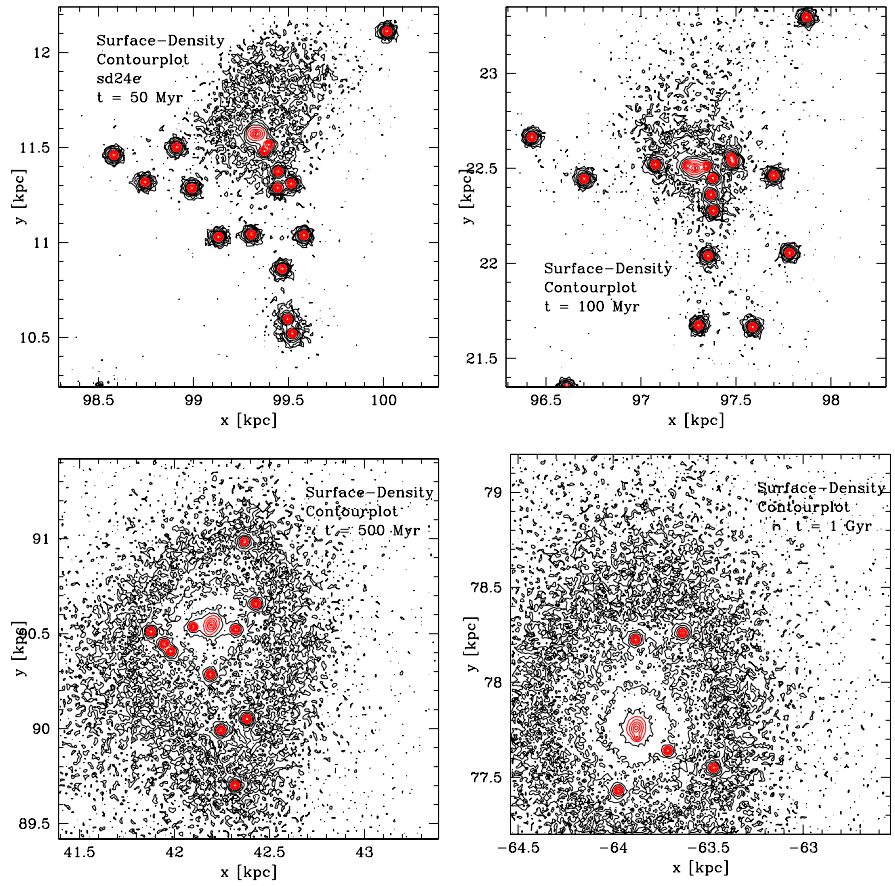

Figure 11. Surface-density contour plots (resolution $(10\ \mathrm{pc})^2$) of a simulation with $\alpha = 0.02$ and $D = 100$ kpc. The crossing time of the super-cluster is 108.4 Myr.

diagram (Fig. 3 in Ferguson & Binggeli 1994). Such objects evolve into dSph-like systems in a periodic tidal field (Fig. 13 in Kroupa 1997; Fig. 2 in Kroupa 1998b). More massive and extended merger-objects can, of course, be obtained by suitable choices of $R_{\rm pl}^{\rm sc}$ and $M_{\rm sc}$, but we defer a more detailed discussion of this to the future.

4. Conclusions

We have performed a set of self-consistent dynamical models of clusters of twenty gas-free star clusters, as they have been recently observed in the Antennae galaxies. For all our models, a central merger object

formed out of a large fraction of the single clusters. As long as the super-cluster is smaller than its tidal radius, almost all clusters merge.

For our choice of parameters (5 kpc $\leq D \leq$ 100 kpc and 300 pc $\leq R_{\rm cut}^{\rm sc} \leq$ 1.8 kpc) the merger process does not depend significantly on the two main dimensionless parameters of the problem, the tidal field strength relative to the super-cluster concentration (β) and the relative concentration of the super-clusters and the individual clusters (α). The cluster merging process cannot be modelled by a sequence of two-body merger events, but is a "collective" interaction, where the first passage ("encounter") of a cluster through the dense central region of the super-cluster leads to the assimilation into a growing merger object. The timescale of the merging process is the same (measured in internal crossing times of the super-cluster $T_{\rm cr}^{\rm sc}$) for all models. Measuring time in years shows that high α calculations form the merger object within very short times ($\approx$ 50 Myr), while for extended clusters (low α) this process can take up to 1 Gyr or even longer.

While for very strong tidal fields the tidal mass loss as e.g. discussed by Baumgardt (1998) dominates and merging processes are suppressed, and for the limit where the individual clusters approach point masses the merging is suppressed as well, our parameter range, which is consistent with the observations, always allows for the quick merger scenario on a few crossing time scales. Tidal mass loss is only a secondary effect for part of our parameter space (stronger tidal field) due to a slight reduction of the number of clusters available for merging. The number of merged clusters $n_{\rm m}$ decreases linearly with β if β becomes larger than 1.0.

We do not claim that our process of forming dwarf galaxies is the only possible way how these objects form, but at least it is one possible way to explain the existence of low-mass dwarf galaxies in the vicinity of large "normal" galaxies like our Milky Way. In addition, some "side-effects" can be explained by our models. It takes very long until all clusters finally end up in the merger object for low values of α. Such systems could account for a high specific globular cluster frequency found in dwarf spheroidal galaxies. Our models develop tidal tails which spread along the orbit of the dwarf galaxy. Surviving escaped star clusters are also found on the orbit. This is similar to what is observed for the Sagittarius dwarf spheroidal galaxy.

Acknowledgements

Part of this project (parallelisation of the code, use of high-performance computing power) was carried out at the Edinburgh Parallel Comput-

ing Centre (EPCC) by the TRACS-programme. The TRACS-programme is a scheme of the European Community (Access to Research Infrastructure action of the Improving Human Potential Programme; contract No HPRI-1999-CT-00026) which allows young Phd- or postdoc scientist to learn parallel computing, offering computing time and support for their projects. MF thanks the staff of EPCC for their support. We also acknowledge the insightful discussions with Prof. D.C. Heggie of the Department of Mathematics & Statistics at the University of Edinburgh.

References

Aarseth, S.J., Fall, S.M., (1980) ApJ, **236** 43.
Aguilar, L.A., White, S.D.M., (1985) ApJ, **295**, 374.
Baumgardt, H., (1998) A&A, **330**, 480.
Binney, J., Tremaine, S., (1987) "Galactic Dynamics", Princeton Univ. Press.
Duc, P.-A., Brinks, E., Springel, V., Pichardo, B., Weilbacher, P., Mirabel, I.F., (2000) AJ, **120**, 1238.
Fellhauer, M., Kroupa, P., Baumgardt, H., Bien, R., Boily, C.M., Spurzem, R., Wassmer, N., (2000) NewA, **5**, 305.
Fellhauer, M., Kroupa, P., (2000) ASP Conf. Ser., **211**, 241.[1]
Fellhauer, M., (2001) PhD-thesis Ruprecht-Karls University, Heidelberg, Germany; Shaker, Aachen, Germany.
Ferguson, H.C., Binggeli, B., (1994) A&ARev., **6**, 67.
Gallagher, S.C., Hunsberger, S.D., Charlton, J.C., Zaritsky, D., (2000) ASP Conf. Ser., **211**, 247.[1]
Gerhard, O.E., Fall, S.M., (1983) MNRAS, **203**, 1253.
Grebel, E.K., (2000) ASP Conf. Ser., **211**, 262.[1]
Hirashita, H., Kamaya, H., Takeuchi, T.T., (2000) PASJ, **51**, 12.
Hunsberger, S.D., (1997) BAAS, **29**, 1406.
Hunsberger, S.D., Gallagher, S.D., Charlton, J.C., Zaritsky, D., (2000) ASP Conf. Ser., **211**, 254.[1]
Klessen, R.S., Kroupa, P., (1998) ApJ, **498**, 143.
Kleyna, J., Geller, M., Kenyon, S., Kurtz, M., (1999) AJ, **117**, 1275.
Kroupa, P., (1997) NewA, **2**, 139.
Kroupa, P., (1998) MNRAS, **300**, 200.
Kroupa, P., (1998b) in "The Magellanic Clouds and other Dwarf Galaxies" eds. T. Richtler, J.M. Braun, Shaker, Aachen, Germany, (astro-ph/9804255).
Makino, J., Hut, P., (1997) ApJ, **481**, 83.
Martinez-Delgado, D., Apaicio, A., Gomez-Flechoso, M.A., (2000) to appear in Proceeding of the Euroconference "The evolution of Galaxies. I. Observational Clues", Granada May 2000. astro-ph/0009066
Mateo, M., (1998) ARAA, **36**, 435.
Miller, B.W., Whitmore, B.C., Schweizer, F., Fall, S.M., (1997) AJ, **114**, 2381.
Spitzer, L., Jr., (1958) ApJ, **127**, 17.
Spitzer, L., Jr., (1987) "Dynamical Evolution of Globular Clusters", Princeton University Press.
Struck, C., Phys. Rep., (1999) **321**, 1.

Whitmore, B.C., Schweizer, F., (1995) AJ, **109**, 960.
Whitmore, B.C., Schweizer, F., (1995) AJ, **109**, 1412.
Whitmore, B.C., Zhang, Q., Leitherer, C., Fall, S.M., (1999) AJ, **118**, 1551.
Zhang, Q., Fall, S.M., (1999) ApJL, **527**, 81L.

[1]: ASP Conf. Ser. 211: Proceedings of the workshop "Massive Stellar Clusters" held in Strasbourg Nov. 1999; eds. A. Lancon, C.M. Boily